

Joint Scattering Environment Sensing and Channel Estimation for Integrated Sensing and Communication

Wenkang Xu, Yongbo Xiao, An Liu and Minjian Zhao
College of Information Science and Electronic Engineering, Zhejiang University

Abstract—This paper considers an integrated sensing and communication system, where some radar targets also serve as communication scatterers. A location domain channel modeling method is proposed based on the position of targets and scatterers in the scattering environment, and the resulting radar and communication channels exhibit a partially common sparsity. By exploiting this, we propose a joint scattering environment sensing and channel estimation scheme to enhance the target/scatterer localization and channel estimation performance simultaneously. Specifically, the base station (BS) first transmits downlink pilots to sense the targets in the scattering environment. Then the user transmits uplink pilots to estimate the communication channel. Finally, joint scattering environment sensing and channel estimation are performed at the BS based on the reflected downlink pilot signal and received uplink pilot signal. A message passing based algorithm is designed by combining the turbo approach and the expectation maximization method. The advantages of our proposed scheme are verified in the simulations.

Index Terms—Integrated sensing and communication, location domain, scattering environment sensing, channel estimation.

I. INTRODUCTION

Radar sensing and wireless communication systems have been developed independently for decades, and they are usually designed separately. However, there are many similarities between sensing and communication systems, such as signal processing algorithms, hardware architecture and channel characteristics [1], [2]. The sensing and communication functionalities are expected to mutually assist each other by leveraging these similarities.

We focus on the scattering environment in massive multi-input multi-output (MIMO) Orthogonal Frequency Division Multiplexing (OFDM) integrated sensing and communication (ISAC) systems, which reflects an interesting similarity between radar sensing and communication in terms of channel characteristics. The scattering environment includes two subsets, i.e., radar targets and communication scatterers. However, some radar targets also serve as communication scatterers in many cases. In an ISAC scenario for vehicle networks, for instance, the BS needs to localize vehicles and obstacles on the road and broadcast the sensing data to every vehicle to realize automatic obstacle avoidance and route planning. In this case, some vehicles and obstacles also contribute to communication paths for neighboring vehicles. Due to the partial overlap between radar targets and communication scatterers, radar and communication channels will exhibit a partially common sparsity in some sparse domains.

Recently, some related works have also exploited this similarity to achieve target sensing and channel estimation in

ISAC systems. In [3], based on the assumption that targets also serve as scatterers for the communication signal, the authors proposed a novel target sensing and channel estimation scheme. However, the target sensing and channel estimation were carried out independently. In [4], the authors merged target sensing and channel estimation into a single procedure under the assumption that radar targets and communication scatterers partially overlapped. The authors in [5] studied an application of ISAC for unmanned aerial vehicle (UAV) networks, in which a UAV communicated with the terrestrial station while other UAVs and obstacles were viewed as radar targets. In [6], [7], each radar target was also a communication receiver, and a two-step approach was proposed to estimate the target location and the line-of-sight (LoS) channel path. However, to the best of our knowledge, the existing works did not consider joint scattering environment sensing and channel estimation in MIMO-OFDM ISAC systems, where scattering environment sensing refers to the joint localization of radar targets and communication scatterers.

In this paper, we consider a time-division duplex (TDD) massive MIMO-OFDM ISAC system and propose a joint scattering environment sensing and channel estimation scheme. A novel location domain sparse representation of radar and communication channels is introduced, which is suitable to perform the joint localization of radar targets and communication scatterers. The partially common sparsity of the location domain channels is exploited to improve both target/scatterer localization and channel estimation performance. However, some non-ideal factors, such as time offset and user localization error, seriously degrade sensing and estimation performance. In order to mitigate their impact, the accurate estimation of these non-ideal factors is taken into account in the algorithm design. A scattering environment aware turbo sparse Bayesian inference (SEA-Turbo-SBI) algorithm is designed to solve the problem by combining the turbo approach and the expectation maximization (EM) method.

II. SYSTEM MODEL

A. Architecture of the ISAC System

Consider a TDD massive MIMO-OFDM ISAC system, where one BS equipped with $M \gg 1$ antennas serves a mobile user equipped with one antenna while sensing the scattering environment, as illustrated in Fig. 1. The BS transmits downlink pilots to sense the targets in the scattering environment, and then the user transmits uplink pilots to estimate the communication channel. Suppose there are a total number of

K targets and L communication scatterers in the scattering environment. As discussed above, there might be some overlap between targets and communication scatterers. The user is located at $\mathbf{p}_u = [p^x, p^y]^T$ in a two-dimensional (2-D) area \mathcal{R} . The BS is located at a known position $\mathbf{p}_b = [\tilde{p}^x, \tilde{p}^y]^T$. Let $\mathbf{p}_k^r = [p_k^{r,x}, p_k^{r,y}]^T$ and $\mathbf{p}_l^c = [p_l^{c,x}, p_l^{c,y}]^T$ be the coordinates of the k -th target and the l -th communication scatterer. We assume that the BS has some prior information about the user location based on the Global Positioning System (GPS) or the previous user localization result.

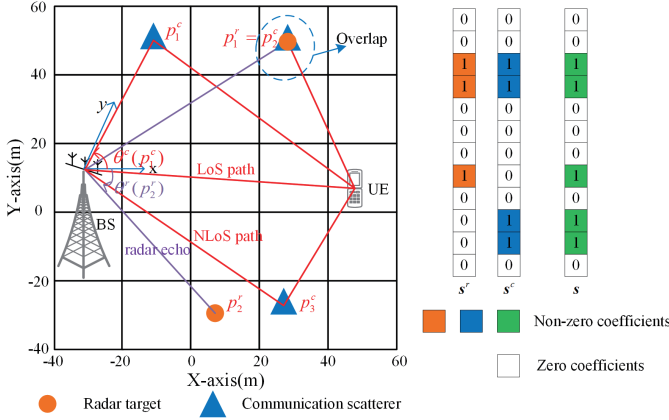


Fig. 1. Illustration of radar and communication channels.

B. Reflected Downlink Pilot Signal

Target sensing aims at detecting the presence of the target and estimating the target location. To achieve this, on the n -th subcarrier, the BS transmits a downlink pilot $\mathbf{v}_n^r \in \mathbb{C}^{M \times 1}$, and the received signal reflected from the targets can be expressed as

$$\mathbf{y}_n^r = \mathbf{H}_n^r \mathbf{v}_n^r + \mathbf{z}_n^r, \quad (1)$$

where $\mathbf{H}_n^r \in \mathbb{C}^{M \times M}$ denotes the radar channel matrix and \mathbf{z}_n^r is the additive white Gaussian noise (AWGN) with variance $(\sigma_z^r)^2$. Let $\theta^r(\mathbf{p}_k^r)$ and $\tau^r(\mathbf{p}_k^r)$ represent the angle of arrival (AoA) and delay of the k -th target, respectively, which are related to the position of the BS and the k -th target through

$$\theta^r(\mathbf{p}_k^r) = \arctan\left(\frac{p_k^{r,y} - \tilde{p}^y}{p_k^{r,x} - \tilde{p}^x}\right) + \pi \cdot \mathbb{1}(p_k^{r,x} < \tilde{p}^x),$$

$$\tau^r(\mathbf{p}_k^r) = \frac{2 \|\mathbf{p}_b - \mathbf{p}_k^r\|}{c},$$

where the angle is calculated anticlockwise and with respect to the x -axis, $\mathbb{1}(E)$ is the indication function, which means that if the logical expression E is true, then $\mathbb{1}(E) = 1$, $\|\cdot\|$ denotes the Euclidean norm of the given vector, and c denotes the speed of light. Then the radar channel matrix can be modeled as

$$\mathbf{H}_n^r = \sum_{k=0}^K x_k^r e^{-j2\pi n f_0 (\tau^r(\mathbf{p}_k^r))} \mathbf{a}(\theta^r(\mathbf{p}_k^r)) \mathbf{a}^T(\theta^r(\mathbf{p}_k^r)), \quad (2)$$

where x_k^r represents radar cross section of the k -th target, f_0 is the subcarrier interval, and $\mathbf{a}(\theta) \in \mathbb{C}^{M \times 1}$ denotes the array

response vector at the BS. For the special case of a uniform linear array (ULA), we have

$$\mathbf{a}(\theta) = \frac{1}{\sqrt{M}} \left[1, e^{j\pi \sin \theta}, \dots, e^{j(M-1)\pi \sin \theta} \right]^T.$$

Note that in (2), we treat the user as the 0-th target and define $\mathbf{p}_0^r \triangleq \mathbf{p}_u$. If the BS can “see” the user through the radar echo signal, we have $x_0^r > 0$. In this case, the echo signal also directly provides some additional information to assist in locating the user’s position.

C. Received Uplink Pilot Signal

On the n -th subcarrier, the user transmits an uplink pilot $u_n^c \in \mathbb{C}$ and then the BS receives the signal, which can be expressed as

$$\mathbf{y}_n^c = \mathbf{h}_n^c u_n^c + \mathbf{z}_n^c, \quad (3)$$

where $\mathbf{h}_n^c \in \mathbb{C}^{M \times 1}$ denotes the communication channel vector, \mathbf{z}_n^c is the AWGN with variance $(\sigma_z^c)^2$.

Assume that there are $(L+1)$ paths for the communication channel, i.e., one LoS path and L non-LoS (NLoS) paths. For convenience, we define the LoS path as the 0-th channel path and treat the user as the 0-th communication scatterer with its position $\mathbf{p}_0^c \triangleq \mathbf{p}_u$. Let $\theta^c(\mathbf{p}_l^c)$ and $\tau^c(\mathbf{p}_l^c, \mathbf{p}_u)$ represent the AoA and relative delay of the l -th channel path, respectively, which are related to the position of the BS, the user, and the l -th communication scatterer through

$$\theta^c(\mathbf{p}_l^c) = \arctan\left(\frac{p_l^{c,y} - \tilde{p}^y}{p_l^{c,x} - \tilde{p}^x}\right) + \pi \cdot \mathbb{1}(p_l^{c,x} < \tilde{p}^x),$$

$$\tau^c(\mathbf{p}_l^c, \mathbf{p}_u) = \frac{\|\mathbf{p}_b - \mathbf{p}_l^c\|}{c} + \frac{\|\mathbf{p}_u - \mathbf{p}_l^c\|}{c} - \frac{\|\mathbf{p}_b - \mathbf{p}_u\|}{c}.$$

Then the communication channel vector can be expressed as

$$\mathbf{h}_n^c = \sum_{l=0}^L x_l^c e^{-j2\pi n f_0 (\tau^c(\mathbf{p}_l^c, \mathbf{p}_u) + \tau_o)} \mathbf{a}(\theta^c(\mathbf{p}_l^c)), \quad (4)$$

where x_l^c denotes the complex gain of the l -th channel path and τ_o is the time offset caused by the timing synchronization error at the BS.

The non-ideal factors of time offset and user localization error will cause localization ambiguity for the communication scatterers and degrade the performance of communication channel estimation. We will elaborate on how to estimate these non-ideal factors based on the EM method in Section IV.

III. SPARSE BAYESIAN INFERENCE FORMULATION

In this section, we first obtain a sparse representation of the radar and communication channels in the location domain. Then, we introduce a sparse prior model to capture the partially common sparsity of the radar and communication channels. Finally, we formulate the joint scattering environment sensing and channel estimation problem as a sparse Bayesian inference problem.

A. A Location Domain Sparse Representation of Channels

It is difficult to directly estimate the position of targets and communication scatterers through maximum a posteriori

(MAP) method because the optimization problem is non-convex and has a lot of local optima. To solve this issue, we introduce a grid-based solution to obtain a sparse representation of the channels for better sensing and estimation performance. Specifically, we define a 2-D uniform grid $\{\bar{\mathbf{r}}_1, \dots, \bar{\mathbf{r}}_Q\} \subset \mathcal{R}$ of $Q \gg K + L$ positions, as illustrated in Fig. 1.

In practice, the true positions usually do not lie exactly on the Q discrete position grid points. To get around this problem, one common solution is to introduce a dynamic position grid, denoted by $\mathbf{r} = [\mathbf{r}_1; \dots; \mathbf{r}_Q]$, instead of only using a fixed position grid. In this case, there always exists an \mathbf{r}^* that covers the true position of all targets and communication scatterers. In general, the uniform grid is chosen as the initial point for \mathbf{r} in the algorithm, which makes it easier to find a near-optimal solution for the MAP estimation problem.

Then we define the sparse basis with a dynamic position grid for the radar and communication channels as

$$\mathbf{A}(\mathbf{r}, \mathbf{p}_u) \triangleq [\mathbf{a}(\theta^r(\mathbf{p}_u)), \tilde{\mathbf{A}}(\mathbf{r})] \in \mathbb{C}^{M \times (Q+1)},$$

where

$$\tilde{\mathbf{A}}(\mathbf{r}) \triangleq [\mathbf{a}(\theta^r(\mathbf{r}_1)), \dots, \mathbf{a}(\theta^r(\mathbf{r}_Q))].$$

The sparse representation of the radar channel matrix and the communication channel vector on the n -th subcarrier corresponding to (2) and (4) are respectively given by

$$\mathbf{H}_n^r = \mathbf{A}(\mathbf{r}, \mathbf{p}_u) \mathbf{D}_n^r \text{diag}(\mathbf{x}^r) \mathbf{A}^T(\mathbf{r}, \mathbf{p}_u), \quad (5)$$

$$\mathbf{h}_n^c = \mathbf{A}(\mathbf{r}, \mathbf{p}_u) \mathbf{D}_n^c \mathbf{x}^c, \quad (6)$$

where $\mathbf{x}^r \in \mathbb{C}^{(Q+1) \times 1}$ and $\mathbf{x}^c \in \mathbb{C}^{(Q+1) \times 1}$ are called the location domain sparse radar and communication channel vectors, \mathbf{D}_n^r and \mathbf{D}_n^c are diagonal matrices, with the 0-th diagonal elements being $e^{-j2\pi n f_0 \tau^r(\mathbf{p}_u)}$ and $e^{-j2\pi n f_0 \tau_o}$, respectively, and the q -th diagonal elements being $e^{-j2\pi n f_0 \tau^r(\mathbf{r}_q)}$ and $e^{-j2\pi n f_0 (\tau^c(\mathbf{r}_q, \mathbf{p}_u) + \tau_o)}$, respectively, for $q = 1, \dots, Q$. \mathbf{x}^r and \mathbf{x}^c only have a few non-zero elements corresponding to the position of targets and communication scatterers, respectively. Specifically, the q -th element of \mathbf{x}^r , denoted by x_q^r , represents the complex reflection coefficient of a target lying in the position \mathbf{r}_q . The q -th element of \mathbf{x}^c , denoted by x_q^c , represents the complex channel gain of the channel path with the corresponding communication scatterer lying in the position \mathbf{r}_q .

B. A Sparse Prior Model for the Partially Common Sparsity

We introduce a sparse prior model to describe the partially common sparsity of the location domain radar and communication channels. We define the support vectors of the radar channel and communication channel as $\mathbf{s}^r \triangleq [s_0^r, \dots, s_Q^r]^T$ and $\mathbf{s}^c \triangleq [s_0^c, \dots, s_Q^c]^T$, respectively. If there is a radar target (communication scatterer) around the q -th position grid \mathbf{r}_q , we have $s_q^r = 1$ ($s_q^c = 1$). Otherwise, we have $s_q^r = 0$ ($s_q^c = 0$). Note that $s_0^r = 1$ indicates that the BS can “see” the mobile user through the radar echo signal and $s_0^c = 1$ indicates that the LoS path exists.

The elements of \mathbf{x}^r and \mathbf{x}^c are independent conditioned on the support vectors \mathbf{s}^r and \mathbf{s}^c , and the conditional distributions are given by

$$p(x_q^r | s_q^r) = (1 - s_q^r) \delta(x_q^r) + s_q^r \mathcal{CN}(x_q^r; 0, (\sigma_q^r)^2), \quad (7a)$$

$$p(x_q^c | s_q^c) = (1 - s_q^c) \delta(x_q^c) + s_q^c \mathcal{CN}(x_q^c; 0, (\sigma_q^c)^2), \quad (7b)$$

where $\delta(\cdot)$ is the Dirac Delta function, $(\sigma_q^r)^2$ and $(\sigma_q^c)^2$ denote the conditional variance of x_q^r and x_q^c , respectively.

Then we introduce a joint support vector $\mathbf{s} \triangleq [s_0, \dots, s_Q]^T$ with $s_q = s_q^r \vee s_q^c$ to represent the common positions of the radar targets and communication scatterers, where \vee means the logical “or” operator. The joint distribution of support vectors \mathbf{s}^r , \mathbf{s}^c and \mathbf{s} can be expressed as

$$\begin{aligned} p(\mathbf{s}^r, \mathbf{s}^c, \mathbf{s}) &= p(\mathbf{s}^r | \mathbf{s}) p(\mathbf{s}^c | \mathbf{s}) p(\mathbf{s}) \\ &= \prod_q p(s_q^r | s_q) \prod_q p(s_q^c | s_q) \prod_q p(s_q), \end{aligned} \quad (8)$$

where

$$p(s_q^r | s_q) = (1 - s_q) \delta(s_q^r) + s_q \left(\rho_r^{s_q} (1 - \rho_r)^{1-s_q} \right), \quad (9a)$$

$$p(s_q^c | s_q) = (1 - s_q) \delta(s_q^c) + s_q \left(\rho_c^{s_q} (1 - \rho_c)^{1-s_q} \right), \quad (9b)$$

$$p(s_q) = \lambda^{s_q} (1 - \lambda)^{1-s_q}, \quad (9c)$$

where λ denotes the sparsity level of \mathbf{s} , ρ_r and ρ_c represent the probability of $s_q^r = 1$ and $s_q^c = 1$ conditioned on $s_q = 1$, respectively, and the value of $(\rho_r + \rho_c - 1)$ represents how much the targets and communication scatterers overlap.

With the sparse prior model discussed above, the joint distribution of all random variables can be expressed as

$$\begin{aligned} &p(\mathbf{s}^r, \mathbf{s}^c, \mathbf{s}, \mathbf{x}^r, \mathbf{x}^c) \\ &= p(\mathbf{s}^r, \mathbf{s}^c, \mathbf{s}) \prod_q p(x_q^r | s_q^r) \prod_q p(x_q^c | s_q^c). \end{aligned} \quad (10)$$

C. Sparse Bayesian Inference with Uncertain Parameters

Using the location domain sparse representation of radar channel and communication channel in (5) and (6), the reflected downlink pilot signal and received uplink pilot signal on all available subcarriers can be expressed as

$$\mathbf{y}^r = \mathbf{\Phi}^r(\mathbf{r}, \mathbf{p}_u) \mathbf{x}^r + \mathbf{z}^r, \quad (11a)$$

$$\mathbf{y}^c = \mathbf{\Phi}^c(\mathbf{r}, \mathbf{p}_u, \tau_o) \mathbf{x}^c + \mathbf{z}^c, \quad (11b)$$

where \mathbf{y}^r , \mathbf{y}^c , \mathbf{z}^r , and \mathbf{z}^c are respectively given by

$$\mathbf{y}^r \triangleq [(\mathbf{y}_1^r)^T, \dots, (\mathbf{y}_N^r)^T]^T \in \mathbb{C}^{MN \times 1},$$

$$\mathbf{y}^c \triangleq [(\mathbf{y}_1^c)^T, \dots, (\mathbf{y}_N^c)^T]^T \in \mathbb{C}^{MN \times 1},$$

$$\mathbf{z}^r \triangleq [(\mathbf{z}_1^r)^T, \dots, (\mathbf{z}_N^r)^T]^T \in \mathbb{C}^{MN \times 1},$$

$$\mathbf{z}^c \triangleq [(\mathbf{z}_1^c)^T, \dots, (\mathbf{z}_N^c)^T]^T \in \mathbb{C}^{MN \times 1},$$

$\Phi^c \in \mathbb{C}^{MN \times (Q+1)}$ denotes the communication measurement matrix, which is given by

$$\Phi^c = \begin{bmatrix} u_1^c \mathbf{A}(\mathbf{r}, \mathbf{p}_u) \mathbf{D}_1^c \\ \vdots \\ u_N^c \mathbf{A}(\mathbf{r}, \mathbf{p}_u) \mathbf{D}_N^c \end{bmatrix},$$

and $\Phi^r \in \mathbb{C}^{MN \times (Q+1)}$ denotes the radar measurement matrix that consists of the $((q-1)Q + q)$ -th column of $\tilde{\Phi}^r \in \mathbb{C}^{MN \times (Q+1)^2}$ for $q = 1, \dots, (Q+1)$, where

$$\tilde{\Phi}^r = \begin{bmatrix} \left((v_1^r)^T \mathbf{A}(\mathbf{r}, \mathbf{p}_u) \right) \otimes \left(\mathbf{A}(\mathbf{r}, \mathbf{p}_u) \mathbf{D}_1^r \right) \\ \vdots \\ \left((v_N^r)^T \mathbf{A}(\mathbf{r}, \mathbf{p}_u) \right) \otimes \left(\mathbf{A}(\mathbf{r}, \mathbf{p}_u) \mathbf{D}_N^r \right) \end{bmatrix},$$

where \otimes means the Kronecker product operator. For convenience, we combine (11a) and (11b) into a linear observation model as

$$\mathbf{y} = \Phi(\boldsymbol{\xi}) \mathbf{x} + \mathbf{z}, \quad (12)$$

where $\boldsymbol{\xi} \triangleq \{\mathbf{r}, \mathbf{p}_u, \tau_o\}$ is the collection of sensing parameters, $\mathbf{y} \triangleq [(\mathbf{y}^r)^T, (\mathbf{y}^c)^T]^T$, $\mathbf{x} \triangleq [(\mathbf{x}^r)^T, (\mathbf{x}^c)^T]^T$, $\mathbf{z} \triangleq [(\mathbf{z}^r)^T, (\mathbf{z}^c)^T]^T$, and $\Phi(\boldsymbol{\xi}) \triangleq \text{BlockDiag}(\Phi^r, \Phi^c)$.

Let $p(\boldsymbol{\xi})$ represents the known prior distribution of the sensing parameters (we can assume uniform distribution if unknown). Our primary goal is to estimate the channel vector \mathbf{x} , the support set $\{s^r, s^c\}$, and the uncertain parameters $\boldsymbol{\xi}$ given observation \mathbf{y} in model (12). To be specific, for given $\boldsymbol{\xi}$, we aim at computing the conditional marginal posteriors, i.e., $p(x_q^r | \mathbf{y}; \boldsymbol{\xi})$, $p(x_q^c | \mathbf{y}; \boldsymbol{\xi})$, $p(s_q^r | \mathbf{y}; \boldsymbol{\xi})$, $p(s_q^c | \mathbf{y}; \boldsymbol{\xi})$, $\forall q$. On the other hand, the uncertain parameters $\boldsymbol{\xi}$ are obtained by the MAP estimator as follows:

$$\boldsymbol{\xi}^* = \arg \max_{\boldsymbol{\xi}} \ln p(\mathbf{y}, \boldsymbol{\xi}). \quad (13)$$

Once we obtain the MAP estimate of $\boldsymbol{\xi}^*$, we can obtain the minimum mean square error (MMSE) estimate of x_q^r as $x_q^{r*} = \int_{x_q^r} x_q^r p(x_q^r | \mathbf{y}; \boldsymbol{\xi}^*)$ and the MAP estimate of s_q^r as $s_q^{r*} = \arg \max_{s_q^r} p(s_q^r | \mathbf{y}; \boldsymbol{\xi}^*)$. The MMSE estimate of x_q^c and the MAP estimate of s_q^c can be obtained in the same way.

However, the corresponding factor graph of the probability model contains loops. Therefore, it is exceedingly challenging to calculate the above conditional marginal posteriors precisely. In the following section, we present the SEA-Turbo-SBI algorithm, which uses the turbo approach to calculate approximate marginal posteriors and applies the EM method to find an approximate solution for (13).

IV. SEA-TURBO-SBI ALGORITHM

The primary goal of the SEA-Turbo-SBI algorithm is to simultaneously maximize $\ln p(\mathbf{y}, \boldsymbol{\xi})$ with respect to the uncertain parameters $\boldsymbol{\xi}$ in (13) and approximately calculate the conditional marginal posteriors. The SEA-Turbo-SBI algorithm, which is based on the EM method, iterates between the next two major steps until convergence.

- **SEA-Turbo-SBI-E Step:** Based on the turbo approach, calculate the approximate marginal posteriors, i.e.,

$p(x_q^r | \mathbf{y}; \boldsymbol{\xi}^i)$, $p(x_q^c | \mathbf{y}; \boldsymbol{\xi}^i)$, $p(s_q^r | \mathbf{y}; \boldsymbol{\xi}^i)$, $p(s_q^c | \mathbf{y}; \boldsymbol{\xi}^i)$, $\forall q$ for given $\boldsymbol{\xi}^i$ in the i -th iteration.

- **SEA-Turbo-SBI-M Step:** Construct a surrogate function for $\ln p(\mathbf{y}, \boldsymbol{\xi})$ based on the approximate marginal posterior $p(\mathbf{x} | \mathbf{y}; \boldsymbol{\xi}^i)$ obtained in the SEA-Turbo-SBI-E Step, then use the gradient ascent method to maximize the surrogate function with respect to $\boldsymbol{\xi}$.

A. SEA-Turbo-SBI-E Step

There are two modules in the SEA-Turbo-SBI-E Step, as illustrated in Fig. 2. Module A performs the linear minimum mean square error (LMMSE) estimation based on the observation \mathbf{y} and extrinsic messages from Module B, whereas Module B is a MMSE estimator that can process the sparse prior information and extrinsic messages from Module A. The two modules iterate until they reach a point of convergence. We omit $\boldsymbol{\xi}$ in $\Phi(\boldsymbol{\xi})$ for simplicity in this subsection because $\boldsymbol{\xi}$ is fixed in the SEA-Turbo-SBI-E Step.

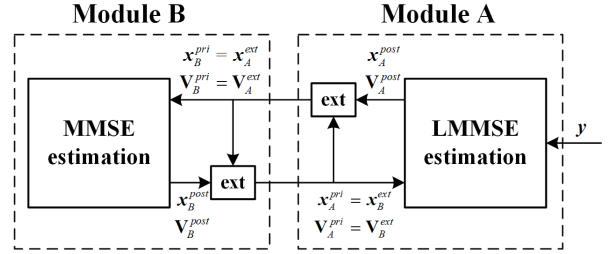


Fig. 2. Illustration of the turbo approach.

1) *Module A with LMMSE Estimation:* We assume that the prior distribution of \mathbf{x} is $\mathcal{CN}(\mathbf{x}; \mathbf{x}_A^{pri}, \mathbf{V}_A^{pri})$, where \mathbf{x}_A^{pri} and \mathbf{V}_A^{pri} are the extrinsic mean and covariance matrix from Module B, respectively. The posterior mean and covariance matrix of the LMMSE estimation are respectively given by

$$\mathbf{x}_A^{post} = \mathbf{V}_A^{post} \left(\left(\mathbf{V}_A^{pri} \right)^{-1} \mathbf{x}_A^{pri} + \frac{\Phi^H \mathbf{y}}{\sigma_z^2} \right), \quad (14)$$

$$\mathbf{V}_A^{post} = \left(\frac{\Phi^H \Phi}{\sigma_z^2} + \left(\mathbf{V}_A^{pri} \right)^{-1} \right)^{-1}. \quad (15)$$

By subtracting the prior information from posterior information, we obtain the extrinsic message from Module A as follows:

$$\begin{aligned} \mathbf{x}_A^{ext} &= \mathbf{V}_A^{ext} \left(\left(\overline{\mathbf{V}}_A^{post} \right)^{-1} \mathbf{x}_A^{post} - \left(\mathbf{V}_A^{pri} \right)^{-1} \mathbf{x}_A^{pri} \right), \\ \mathbf{V}_A^{ext} &= \left(\left(\overline{\mathbf{V}}_A^{post} \right)^{-1} - \left(\mathbf{V}_A^{pri} \right)^{-1} \right)^{-1}, \end{aligned} \quad (16)$$

where $\overline{\mathbf{V}}_A^{post}$ takes each element in the diagonal of matrix \mathbf{V}_A^{post} while setting the non-diagonal elements to be zero.

2) *Module B with Message Passing:* In Module B, we construct a factor graph and derive a message passing algorithm to achieve the MMSE estimator. First of all, a basic assumption is to model the extrinsic mean from Model A as an AWGN observation, i.e.,

$$\mathbf{x}_B^{pri} = \mathbf{x} + \mathbf{w}, \quad (17)$$

where $\mathbf{w} \sim \mathcal{CN}(0, \mathbf{V}_B^{pri})$ is the virtual noise, \mathbf{x}_B^{pri} and \mathbf{V}_B^{pri} are the extrinsic mean and covariance matrix from Module A, which are respectively given by

$$\begin{aligned} \mathbf{x}_B^{pri} &= \mathbf{x}_A^{ext} \triangleq \left[\left(\mathbf{x}_B^{r,pri} \right)^T, \left(\mathbf{x}_B^{c,pri} \right)^T \right]^T, \\ \mathbf{V}_B^{pri} &= \mathbf{V}_A^{ext} \triangleq \text{BlockDiag} \left(\mathbf{V}_B^{r,pri}, \mathbf{V}_B^{c,pri} \right). \end{aligned}$$

The factor graph of $p(\mathbf{x}_B^{r,pri}, \mathbf{x}_B^{c,pri}, \mathbf{x}^r, \mathbf{x}^c, \mathbf{s}, \mathbf{s}^r, \mathbf{s}^c)$, denoted by \mathcal{G}_B , is shown in Fig. 3, where the factor nodes are defined as follows:

$$\begin{aligned} g_q^t &\triangleq \mathcal{CN}(x_q^t; x_{B,q}^{t,pri}, v_{B,q}^{t,pri}), t \in \{r, c\}, \forall q, \\ f_q^t &\triangleq p(x_q^t | s_q^t), t \in \{r, c\}, \forall q, \\ \eta_q^t &\triangleq p(s_q^t | s_q), t \in \{r, c\}, \forall q, \\ h_q &\triangleq p(s_q), \forall q, \end{aligned}$$

where $x_{B,q}^{t,pri}$ denotes the q -th element of $\mathbf{x}_B^{t,pri}$ and $v_{B,q}^{t,pri}$ denotes the q -th diagonal element of $\mathbf{V}_B^{t,pri}$.

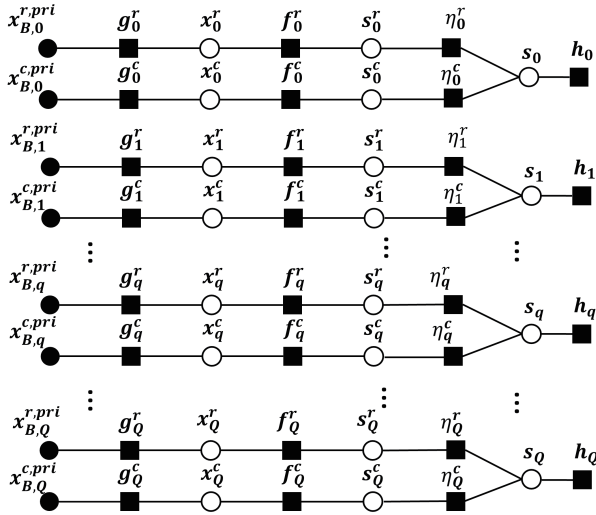


Fig. 3. The factor graph of the joint distribution of all variables.

We use the sum-product rule to derive messages over the factor graph \mathcal{G}_B in Fig. 3. Due to the tree-type structure of \mathcal{G}_B , the derivation of all messages is relatively easy (similar to the message passing in Appendix A of [4]) so that we omit it for simplicity. The approximate posterior distributions can be calculated as

$$\hat{p}(x_q^t | \mathbf{y}) \propto \nu_{f_q^t \rightarrow x_q^t} \times \nu_{x_q^t \rightarrow f_q^t}, t \in \{r, c\}, \forall q, \quad (18)$$

$$\hat{p}(s_q^t | \mathbf{y}) \propto \nu_{f_q^t \rightarrow s_q^t} \times \nu_{s_q^t \rightarrow f_q^t}, t \in \{r, c\}, \forall q, \quad (19)$$

where $\nu_{f_q^t \rightarrow x_q^t}$ and $\nu_{x_q^t \rightarrow f_q^t}$ denote the messages from factor node f_q^t to variable nodes x_q^t and s_q^t , respectively, $\nu_{x_q^t \rightarrow f_q^t}$ and $\nu_{s_q^t \rightarrow f_q^t}$ denote the messages from variable nodes x_q^t and s_q^t to factor node f_q^t , respectively. Based on the the posterior

distributions, the posterior mean and covariance matrix for \mathbf{x}^t , denoted by

$$\begin{aligned} \mathbf{x}_B^{t,post} &\triangleq \left[x_{B,0}^{t,post}, \dots, x_{B,Q}^{t,post} \right]^T, \\ \mathbf{V}_B^{t,post} &\triangleq \text{diag} \left(\left[v_{B,0}^{t,post}, \dots, v_{B,Q}^{t,post} \right] \right), \end{aligned}$$

can be calculated respectively as

$$x_{B,q}^{t,post} = \int_{x_q^t} x_q^t \hat{p}(x_q^t | \mathbf{y}), \quad (20)$$

$$v_{B,q}^{t,post} = \int_{x_q^t} \left| x_q^t - x_{B,q}^{t,post} \right|^2 \hat{p}(x_q^t | \mathbf{y}), \quad (21)$$

for $q = 0, \dots, Q$. Then the extrinsic message from Module B can be calculated as

$$\begin{aligned} \mathbf{x}_B^{ext} &= \mathbf{V}_B^{ext} \left(\left(\mathbf{V}_B^{post} \right)^{-1} \mathbf{x}_B^{post} - \left(\mathbf{V}_A^{pri} \right)^{-1} \mathbf{x}_B^{pri} \right), \\ \mathbf{V}_B^{ext} &= \left(\left(\mathbf{V}_B^{post} \right)^{-1} - \left(\mathbf{V}_B^{pri} \right)^{-1} \right)^{-1}, \end{aligned} \quad (22)$$

where \mathbf{x}_B^{post} and \mathbf{V}_B^{post} are respectively given by

$$\begin{aligned} \mathbf{x}_B^{post} &\triangleq \left[\left(\mathbf{x}_B^{r,post} \right)^T, \left(\mathbf{x}_B^{c,post} \right)^T \right]^T, \\ \mathbf{V}_B^{post} &\triangleq \text{BlockDiag} \left(\mathbf{V}_B^{r,post}, \mathbf{V}_B^{c,post} \right). \end{aligned}$$

B. SEA-Turbo-SBI-M Step

Since there is no close-form expression of $\ln p(\mathbf{y}, \boldsymbol{\xi})$, it is challenging to directly solve the maximization problem in (13). To get around this problem, one common solution is to construct a surrogate function of $\ln p(\mathbf{y}, \boldsymbol{\xi})$ and maximize the surrogate function with respect to $\boldsymbol{\xi}$. Specifically, in the i -th iteration, the surrogate function inspired by the EM method is given by

$$\begin{aligned} Q(\boldsymbol{\xi}; \boldsymbol{\xi}^i) &= \int p(\mathbf{x} | \mathbf{y}; \boldsymbol{\xi}^i) \ln \frac{p(\mathbf{y}, \mathbf{x} | \boldsymbol{\xi})}{p(\mathbf{x} | \mathbf{y}; \boldsymbol{\xi}^i)} d\mathbf{x} + \ln p(\boldsymbol{\xi}) \\ &= -(\sigma_z)^{-2} \left[\|\mathbf{y} - \Phi(\boldsymbol{\xi}) \mathbf{x}^{post}\|^2 \right. \\ &\quad \left. + \text{tr} \left(\Phi(\boldsymbol{\xi}) \mathbf{V}_B^{post} \Phi(\boldsymbol{\xi})^H \right) \right] + \ln p(\boldsymbol{\xi}) + C, \end{aligned} \quad (23)$$

where the posterior mean \mathbf{x}^{post} and covariance matrix \mathbf{V}_B^{post} can be approximated to \mathbf{x}_A^{post} and \mathbf{V}_A^{post} in (14) and (15), respectively, and C is a constant. At the current iterate $\boldsymbol{\xi}^i$, the surrogate function and its gradient satisfy the following properties:

$$Q(\boldsymbol{\xi}; \boldsymbol{\xi}^i) \leq \ln p(\mathbf{y}, \boldsymbol{\xi}), \forall \boldsymbol{\xi}, \quad (24a)$$

$$Q(\boldsymbol{\xi}^i; \boldsymbol{\xi}^i) = \ln p(\mathbf{y}, \boldsymbol{\xi}^i), \quad (24b)$$

$$\frac{\partial Q(\boldsymbol{\xi}; \boldsymbol{\xi}^i)}{\partial \boldsymbol{\xi}} \Big|_{\boldsymbol{\xi}=\boldsymbol{\xi}^i} = \frac{\partial \ln p(\mathbf{y}, \boldsymbol{\xi})}{\partial \boldsymbol{\xi}} \Big|_{\boldsymbol{\xi}=\boldsymbol{\xi}^i}. \quad (24c)$$

Then we need to maximize $Q(\boldsymbol{\xi}; \boldsymbol{\xi}^i)$ to update the next iterate $\boldsymbol{\xi}^{i+1}$. However, it is difficult to find the global optimal solution to the maximizing problem because the function $Q(\boldsymbol{\xi}; \boldsymbol{\xi}^i)$ is

non-convex. Using the gradient ascent method, we can simply obtain the next iterate ξ^{i+1} as

$$\mathbf{r}^{i+1} = \mathbf{r}^i + \varepsilon_r^i \frac{\partial Q(\mathbf{r}^i, \mathbf{p}_u^i, \tau_o^i; \xi^i)}{\partial \mathbf{r}}, \quad (25a)$$

$$\mathbf{p}_u^{i+1} = \mathbf{p}_u^i + \varepsilon_p^i \frac{\partial Q(\mathbf{r}^{i+1}, \mathbf{p}_u^i, \tau_o^i; \xi^i)}{\partial \mathbf{p}_u}, \quad (25b)$$

$$\tau_o^{i+1} = \tau_o^i + \varepsilon_t^i \frac{\partial Q(\mathbf{r}^{i+1}, \mathbf{p}_u^{i+1}, \tau_o^i; \xi^i)}{\partial \tau_o}, \quad (25c)$$

where ε_r^i , ε_p^i and ε_t^i are step sizes determined by the Armijo rule. As a result, we have $\ln p(\mathbf{y}, \xi^{i+1}) \geq Q(\xi^{i+1}; \xi^i) \geq Q(\xi^i; \xi^i) = \ln p(\mathbf{y}, \xi^i)$, which indicates that the function $\ln p(\mathbf{y}, \xi)$ increases strictly until it reaches a stationary point.

V. SIMULATION RESULTS

In the simulations, we consider a $100 \text{ m} \times 100 \text{ m}$ area with a grid resolution of 5 m. The BS is at coordinates $[-50 \text{ m}, 0 \text{ m}]$ and the mobile user is around coordinates $[50 \text{ m}, 0 \text{ m}]$ with a random position offset. We assume that the prior information about the user location is $p^x \sim \mathcal{N}(50, \sigma_p^2/2)$ and $p^y \sim \mathcal{N}(0, \sigma_p^2/2)$, where σ_p^2 is set as 1. There are $K = 9$ radar targets and $L = 10$ communication scatterers within the area. The number of OFDM subcarriers is $N = 1024$ and the subcarrier interval is $f_0 = 30 \text{ kHz}$. Pilot symbols are inserted at intervals of 32 OFDM subcarriers. The BS is equipped with a ULA of $M = 64$ antennas. The time offset τ_o is within $[\frac{-2}{B}, \frac{2}{B}]$, where $B = Nf_0$ denotes the total bandwidth. We compare the performance for orthogonal matching pursuit (OMP) based on separate estimation [8], turbo compressed sensing (Turbo-CS) based on joint estimation with a fixed position grid [9], [10], the proposed SEA-Turbo-SBI based on separate estimation, i.e., without the joint support vector \mathbf{s} , and the proposed SEA-Turbo-SBI based on joint estimation.

Fig. 4 shows the root mean square error (RMSE) of target/scatterer localization versus signal to noise ratio (SNR). It is evident that the proposed SEA-Turbo-SBI based on joint estimation outperforms the baselines in both target and scatterer localization. The normalized mean square error (NMSE) of radar/communication channel estimation versus SNR is shown in Fig. 5. It can be seen that the proposed SEA-Turbo-SBI also achieves the best channel estimation performance. The performance gain between the proposed SEA-Turbo-SBI based on joint estimation and separate estimation reflects our proposed sparse prior model can fully exploit the partially common sparsity of the location domain radar and communication channels.

VI. CONCLUSIONS

We propose a location domain channel modeling method and a joint scattering environment sensing and channel estimation scheme for a massive MIMO-OFDM ISAC system. The SEA-Turbo-SBI algorithm is designed by combining the turbo approach and the EM method, and the proposed sparse prior model can exploit the partially common sparsity of the radar and communication channels. Simulations verified that our proposed scheme can outperform the baselines in both scattering environment sensing and channel estimation.

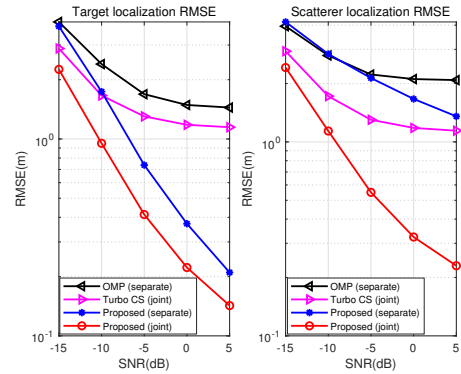


Fig. 4. RMSE of target/scatterer localization versus SNR.

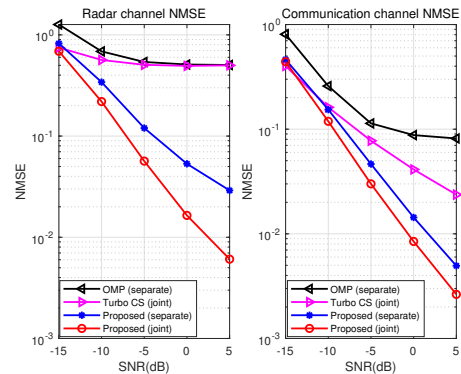


Fig. 5. NMSE of radar/communication channel estimation versus SNR.

REFERENCES

- [1] J. A. Zhang, F. Liu, C. Masouros, R. W. Heath, Z. Feng, L. Zheng, and A. Petropulu, "An overview of signal processing techniques for joint communication and radar sensing," *IEEE J. Sel. Topics Signal Process.*, vol. 15, no. 6, pp. 1295–1315, 2021.
- [2] F. Liu, Y. Cui, C. Masouros, J. Xu, T. X. Han, Y. C. Eldar, and S. Buzzi, "Integrated sensing and communications: Toward dual-functional wireless networks for 6G and beyond," *IEEE J. Sel. Areas Commun.*, vol. 40, no. 6, pp. 1728–1767, 2022.
- [3] F. Liu, C. Masouros, A. P. Petropulu, H. Griffiths, and L. Hanzo, "Joint radar and communication design: Applications, state-of-the-art, and the road ahead," *IEEE Trans. Commun.*, vol. 68, no. 6, pp. 3834–3862, 2020.
- [4] Z. Huang, K. Wang, A. Liu, Y. Cai, R. Du, and T. X. Han, "Joint pilot optimization, target detection and channel estimation for integrated sensing and communication systems," *IEEE Trans. Wireless Commun.*, 2022, doi: 10.1109/TWC.2022.3183621.
- [5] Z. Wan, Z. Gao, S. Tan, and L. Fang, "Joint channel estimation and radar sensing for UAV networks with mmWave massive MIMO," in *IEEE Int. Wireless Commun. Mobile Comput. Conf.*, 2022, pp. 44–49.
- [6] L. Gaudio, M. Kobayashi, G. Caire, and G. Colavolpe, "Joint radar target detection and parameter estimation with MIMO OTFS," in *Proc. IEEE Radar Conf. (RadarConf)*, 2020, pp. 1–6.
- [7] L. Gaudio, M. Kobayashi, G. Caire, and G. Colavolpe, "On the effectiveness of OTFS for joint radar parameter estimation and communication," *IEEE Trans. Wireless Commun.*, vol. 19, no. 9, pp. 5951–5965, 2020.
- [8] J. A. Tropp and A. C. Gilbert, "Signal recovery from random measurements via orthogonal matching pursuit," *IEEE Trans. Inf. Theory*, vol. 53, no. 12, pp. 4655–4666, 2007.
- [9] J. Ma, X. Yuan, and L. Ping, "Turbo compressed sensing with partial DFT sensing matrix," *IEEE Signal Process. Lett.*, vol. 22, no. 2, pp. 158–161, 2015.
- [10] L. Chen, A. Liu, and X. Yuan, "Structured Turbo compressed sensing for massive MIMO channel estimation using a Markov prior," *IEEE Trans. Veh. Technol.*, vol. 67, no. 5, pp. 4635–4639, 2018.